THEORETICAL *PKIKP* MAGNITUDE DETERMINATION

J. JANSKÝ, M. KVASNIČKA

Institute of Geophysics, Charles University, Prague)*

Summary: *The estimation of the theoretical magnitude for deep foci based on the vertica component of medium-period PKIKP waves, Earth model PREM and source spectra is presented. The given graphs are valid for period T ranging from 1·6 s to 10 s, source depth of 25 km to 600 km and distance range of 16 500 km to 19 800 km. A simplified method of representing calibration curves σ is used.*

1. INTRODUCTION

In paper [1] we estimated the theoretical magnitude calibrating curves σ for the vertical component of short-period *PKiKP*/*PKIKP* waves for three values of prevailing periods T (0·8 s, 1·2 s and 1·6 s), epicentral distances of 12 200 km to 19 800 km and source depth h of 25 km to 600 km. The calculation was performed for the Preliminary Reference Earth Model (PREM) [2] using the zero-approximation of the ray theory. The mutual interference of both phases in the distance interval of 13 000 km to 16 000 km for chosen parameters of Gabor's source signal was considered. The interference caused an oscillatory character of the σ. Due to the rapid increase of wave attenuation with decreasing period, the level of σ for individual T was rather different.

In the present paper we study the problem for the broader range of prevailing periods from 1·6 s to 10 s, i.e. we have included the medium periods. Here we encounter two difficulties: a) The inaccuracy of the zero-approximation of the ray theory (in calculating the amplitudes of reflected and refracted waves) in the vicinity of the critical point [3, 4] increases considerably with period; b) The form of oscillation of amplitudes in the interference distance range depends on the prevailing period and changes significantly with T. This is shown in Fig. 1 where we compare σ for interference complex for $T = 3$ s and $T = 6$ s (where Gabor's source time function [5] with $\gamma = 5$ and $\psi = 0$ was used). This effect would require the calculation of calibrating curves σ for the set of prevailing periods T.

We have, therefore, limited our calculation to the calibrating curves of a single *PKIKP* wave branch over a distance range where the travel time differences are so large that the *PKIKP* branch does not interfere with other *PKP* wave branches, or the interference does not influence the value of the maximum of the *PKIKP* pulse (for $\gamma \leqq 5$ in Gabor's signal). The beginning of this distance range depends on period T. Its lower value, corresponding to the lower period $T = 1{\cdot}6$ s, is about 16 500 km. We have, therefore, used this distance value in our calculation. (For comparison, the value for $T = 5$ s is about 17 000 km). The nearest branch here is PKP_1.

On the other hand, we have not restricted ourselves to the calculation of the calibrating curves only, but we have also considered the influence of source spectra on the magnitude estimation. The source spectra can play an important role due to their different form for lower (e.g. $m \leqq 5$) and higher (e.g. $m \geqq 6$) magnitudes.

2. DESCRIPTION OF CALCULATION METHOD

We assume the validity of the formulas

$$m = F\left[\log\left(\bar{A}_0/T\right)_h, T\right], \tag{1}$$

*) Address: Ke Karlovu 3, 121 16 Praha 2

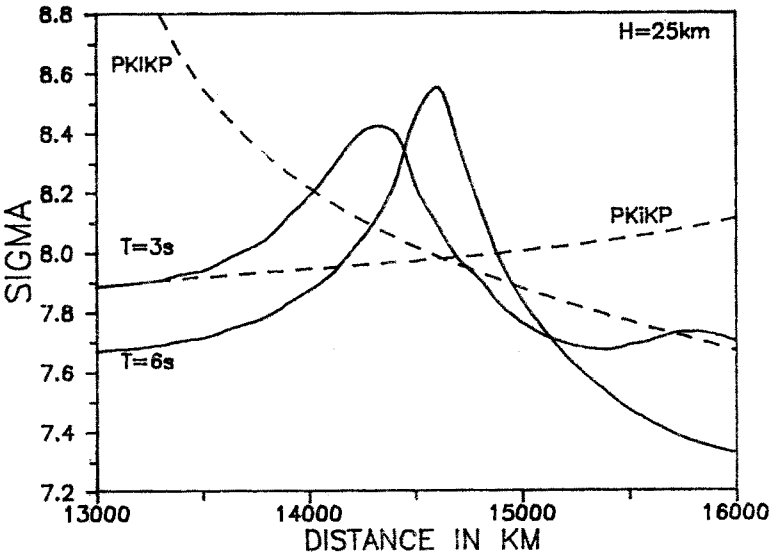

Fig. 1. Comparison of the level and form of calibrating curves σ for interference of *PKiKP* and *PKIKP* branches for $T = 3$ s and $T = 6$ s — full lines ($h = 25$ km, $\gamma = 5$, $\psi = 0$). Corresponding σ for single *PKiKP* and *PKIKP* branches for $T = 3$ s are given by dashed lines. (For PREM.)

where F represents the "source spectral function", $\bar{A}_0 = CA_0\varrho^{1/2}$, A_0 is the displacement amplitude at the source, ϱ the density at the source depth h, T the prevailing period and C the calibrating constant; and

$$\log(\bar{A}_0/T)_h = \log[A(D)/T]_{h=0} + \sigma(D, h, T), \tag{2}$$

where D is the epicentral distance. The calibrating function σ compensates the model influence on displacement amplitude A at epicentral distance D for focal depth h and prevailing period T. We assume the same T at the source and the receiver. (Hereinafter the suffix h has been dropped in the expression $\log[A/T]$.)

The three-parametric function σ can be given in different forms: the function of variables D and h for constant parameter T ($\sigma_T(D, h) = \text{Const.}$, see e.g. [6]), or the function of the variable D for constant parameters T and h ($\sigma_{T,h}(D)$, see e.g. [1]). In this way we get for each T an extra set of calibrating curves.

If σ does not differ much with T (e.g. for greater T) we can use a convenient simplification in the σ representation. Let us divide σ into two parts, namely

$$\sigma(D, h, T) = \sigma^*(D, h, T = \text{Const.}) + \Delta\sigma(D, h, T), \tag{3}$$

where $\Delta\sigma$ (for our range of T, D and h) depends only weakly on D and h. We can thus construct $\Delta\sigma_{D,h}(T)$ for a few combinations of extreme D and h, and $\Delta\sigma$ for other values of D and h can be interpolated from them if necessary. Therefore, just two graphs, i.e. σ^* and $\Delta\sigma$, can cover (with small inaccuracy only) the distribution

of σ. (This method cannot be used for small T, where the signal attenuation changes very quickly.)

The period $T = 6$ s (the middle of our T interval) was chosen for the calculation of σ^*. The $\sigma_h^*(D)$ curves are given in Fig. 2 for h equal to 25, 100, 200, 300, 400,

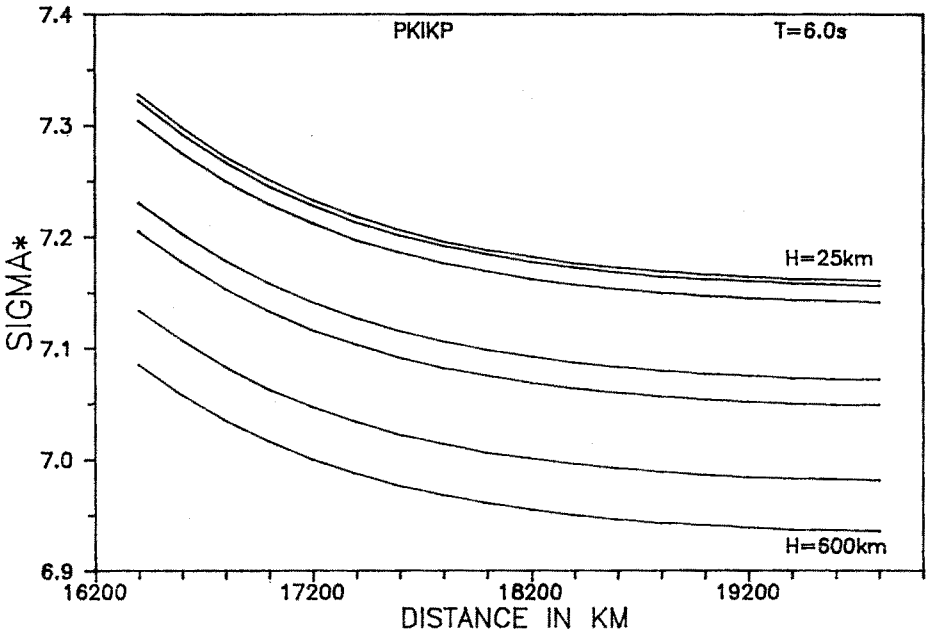

Fig. 2. Theoretical *PKIKP* magnitude calibrating curves σ^* for PREM. $T = 6$ s. The curves are presented in the order: $h = 25$, 100, 200, 300, 400, 500 and 600 km.

500 and 600 km. The corresponding $\Delta\sigma_{D,h}(T)$ curves for combinations: $D = 19\,800$ km, $h = 50$ km – curve "A"; $D = 16\,500$ km, $h = 50$ km or $D = 19\,800$ km, $h = 600$ km – curve "B"; $D = 16\,500$ km, $h = 600$ km – curve "C" are given in Fig. 3. ($|\Delta\sigma|$ increases with increasing D or with decreasing h.) Due to the small differences between the individual curves the interpolation does not seem to be necessary and we recommend to use curve "A" for smaller depths and larger distances, curve "C" for larger depths and smaller distances and curve "B" for other combinations of depth and distance.

Starting with the observed $\log[A(D)/T]$, and using Fig. 2–3 we get $\log(\bar{A}_0/T)$ at the source. The T and $\log(\bar{A}_0/T)$ values allow us to estimate the magnitude m, using the m-isolines in Fig. 4. This figure represents the P-source spectra from [7], modified, in our range of periods, from acceleration spectra to velocity spectra.

The calibration of the σ-axis in Figs 1 and 2 and the $\log(\bar{A}_0/T)$-axis in Fig. 4 was established by using the observational calibrating curve $\sigma(D)$ for medium-period *PV* waves and shallow foci derived by Christoskov et al. [8] (average $T = 6{\cdot}3$ s).

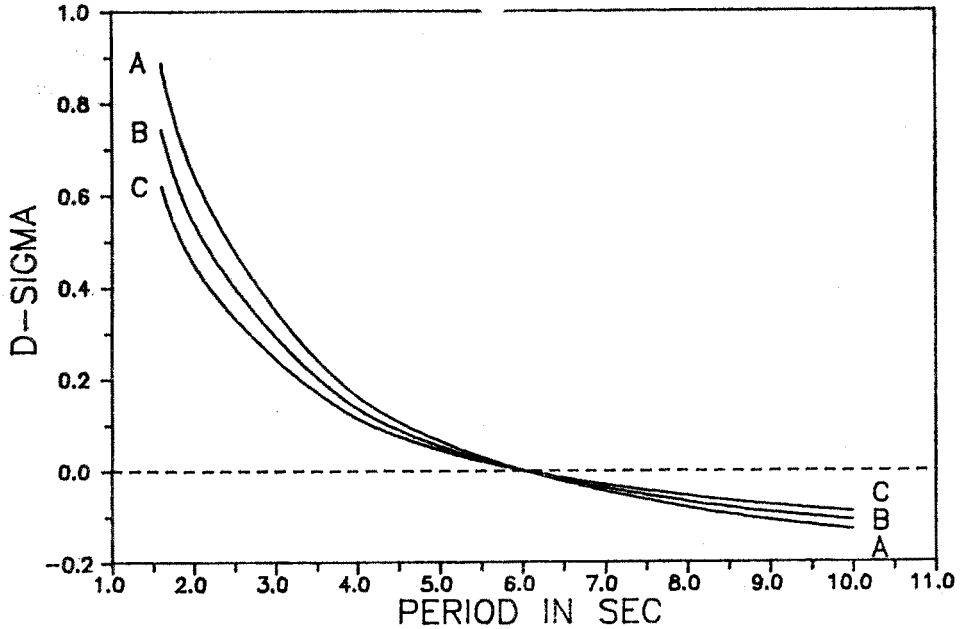

Fig. 3. Theoretical *PKIKP* $\Delta\sigma$ curves for the combination of extreme D and h. Curve "A": $D = 19\,800$ km, $h = 50$ km; Curve "B": $D = 16\,500$ km, $h = 50$ km or $D = 19\,800$ km, $h = 600$ km; Curve "C": $D = 16\,500$ km, $h = 600$ km.

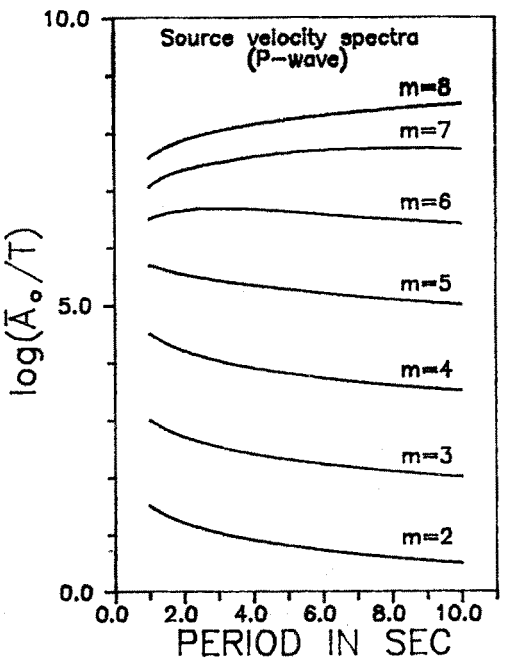

Fig. 4. Source velocity spectra (modified from [7]).

We use their σ-value at $D = 4\,666$ km (i.e. 42°) so that σ^{PKIKP} (17 000 km) = σ^{PV} (4 666 km) + log $[A^{PV}$ (4 666 km)/A^{PKIKP} (17 000 km)], where A^{PV} and A^{PKIKP} are computed values for $h = 50$ km and $T = 6$ s. (In this way our theoretical σ^{PKIKP} are compatible with the theoretical $\sigma^{P}(D, h)$ given in [6] for *PV*-waves and PREM.)

3. DISCUSSION OF RESULTS

For the sake of demonstration, assume that we observe $\log [A(D)/T]_S \cong \log [A(D)/T]_M$ for small magnitudes at a given D (where suffix S denotes short-period and M medium-period waves). After application of the theoretical σ that depends significantly on T, we get $\log [\bar{A}_0/T]_S > \log [\bar{A}_0/T]_M$. According to the source spectra this corresponds to reality for small magnitudes (see Fig. 4) and we can get $m_S \cong m_M$. The routine application of the classical period-independent observational σ (derived originally for medium period [9]) yields $\log [\bar{A}_0/T]_S \cong \log [\bar{A}_0/T]_M$ but also $m_S \cong m_M$, because the source spectra have not been taken into consideration in this case (only the relation $m = \log [\bar{A}_0/T]$ has been used) and the two inaccuracies eliminate one another.

For high magnitudes, where we observe $\log [A(D)/T]_S < \log [A(D)/T]_M$, the application of the theoretical σ and source spectra takes in consideration the lower radiation and higher attenuation of the short-period energy and we can, therefore, still get $m_S \cong m_M$. But if we use the classical period-independent observational σ and do not consider the source spectra, we obtain $m_S < m_M$. This results in underestimation of m from short-period waves for large earthquakes, as frequently observed.

Note here the confirmation of the relation $\sigma_S > \sigma_M$, found recently in [10] for the observational magnitude calibrating curves for *PV*-waves, where $\sigma_S \cong \sigma_M + 0{\cdot}3$ (without consideration of source spectra that would further increase the difference, see this paper).

The level of the magnitude calibrating curves for short-period *PKiKP*/*PKIKP* waves given in [1] was based on observational σ for short-period *PV*-waves [8] (which differs very little from observational σ for medium-period *PV*-waves i.e. $\sigma_S \cong \sigma_M + 0{\cdot}15$ [8]) and the source spectra were not taken in consideration. Therefore, the σ_S in [1] are about half of magnitude unit (0·5) less than σ_S given in this paper.

To compare the mutual level of theoretical medium-period calibrating curves for *PKIKP* waves (for $T = 6$ s) and for *P* waves (for $T = 6{\cdot}3$ s) [6], let us take the shallow foci. For the maximum D used in [6], i.e. for 85° we have $\sigma^{P} = 6{\cdot}95$. For most of the distance range given in Fig. 2 (note that for medium periods the distance range begin at $D > 16\,500$ km) we have $\sigma^{PKIKP} < 7{\cdot}2$. The difference is only 0·25. The *PKIKP* waves are, therefore, strong enough to be used in magnitude determination.

Our paper is based on theoretical calculations. The verification of the results using observational data is necessary, because we did not consider some possible

effects such as the influence of source signal duration, or the possible dependence of the spectra on the source depth. Also the theoretical and observed attenuations should be compare. Note that the directional source radiation pattern was omitted in our calculations.

Acknowledgement: We wish to thank Dr. L. Klimeš, Institute of Geotechnics, Czechoslov. Acad. Sci., for providing us with the Complete Seismic Ray Tracing program.
This work was supported by the IBM Academic Iniciative in Czechoslovakia.

Received 3. 6. 1991

References

[1] M. Kvasnička, J. Janský: Theoretical Short-Period *PKiKP/PKIKP* Magnitude Calibrating Curves for Deep Foci. Studia geoph. et geod., 35 (1991), 203.
[2] A. N. Dziewonski, D. L. Anderson: Preliminary Reference Earth Model. Phys. Earth Planet. Int., 25 (1981), 297.
[3] V. Červený, J. Zahradník: Amplitude Distance Curves of Seismic Body Waves in the Neighborhood of Critical Points and Caustics-A Comparison. Zeitschrift für Geophysik, 38 (1972), 499.
[4] V. Červený, J. Janský: The Amplitude Curves of Seismic Waves at Short Epicentral Distances. Acta Univ. Carolinae-Math. et Phys., No. 1 (1967), 15.
[5] V. Červený: Approximate Expressions for the Hilbert Transform of a Certain Class of Functions and their Application to the Ray Theory of Seismic Waves. Studia geoph. et geod., 20 (1976), 125.
[6] J. Janský, J. Zedník, V. Kárník: Theoretical *PV*—Magnitude Calibrating Curves for Deep. Foci. Studia geoph. et geod., 32 (1988), 264.
[7] J. G. Anderson: Implication of Attenuation for Studies of the Earthquake Source. In: Earthquake Source Mechanics (Eds. S. Das, J. Boatwright, Ch. H. Scholz), Geophysical Monograph 37, Maurice Ewing Volume 6, Amer. Geoph. Union, Washington, D. C., 1986.
[8] L. Christoskov, N. V. Kondorskaya, J. Vaněk: Homogeneous Magnitude System of the Eurasian Continent: *P* Waves. Report SE-18, World Data Center A for Solid Earth Geophysics, Boulder 1979.
[9] B. Gutenberg: Magnitude Determination for Deep-Focus Earthquakes. Bull. Seism. Soc. Am., 35 (1945), 117.
[10] L. V. Christoskov, N. V. Kondorskaya, J. Vaněk: Homogeneous Magnitude System with Unified Level for Usage in Seismological Practice. Studia geoph. et geod., 35 (1991), 221.